Geophys. J. Int. (1996) **125**, 813–829

Upper-crustal seismic velocity heterogeneity as derived from a variety of *P*-wave sonic logs

K. Holliger

Institute of Geophysics, Swiss Federal Institute of Technology, ETH-Hönggerberg, CH-8093 Zürich, Switzerland

Accepted 1996 January 29. Received 1995 November 23; in original form 1995 June 29

SUMMARY

Sonic-log measurements provide detailed 1-D information on the distribution of elastic properties within the upper crystalline crust at scales from about one metre to several kilometres. 10 *P*-wave sonic logs from six upper-crustal drill sites in Europe and North America have been analysed for their second-order statistics. The penetrated lithological sequences comprise Archean volcanic sequences, Proterozoic mafic layered intrusions, and Precambrian to Phanerozoic gneisses and granites. Despite this variability in geological setting, tectonic history, and petrological composition, there are notable similarities between the various data sets: after removing a large-scale, deterministic component from the observed velocity–depth function, the residual velocity fluctuations of all data sets can be described by autocovariance functions corresponding to band-limited self-affine stochastic processes with quasi-Gaussian probability density functions. Depending on the maximum spatial wavelength present in the stochastic part of the data, the deterministic trend can be approximated either by a low-order polynomial best fit or by a moving-average of the original sonic-log data. The choice of the trend has a significant impact on the correlation length and on the standard deviation of the residual stochastic component, but does not affect the Hurst number. For trends defined by low-order polynomial best fits, correlation lengths were found to range from 60 to 160 m, whereas for trends defined by a moving average the correlation lengths are dominated by the upper cut-off wavenumber of the corresponding filter. Regardless of the trend removed, the autocovariance functions of all data sets are characterised by low Hurst numbers of around 0.1–0.2, or equivalently by power spectra decaying as $\sim 1/k$. A possible explanation of this statistical uniformity is that sonic-log fluctuations are more sensitive to the physical state, in particular to the distribution of cracks, than to the petrological composition of the probed rocks.

Key words: borehole geophysics, cracks, fractals, porosity, statistical methods, upper crust.

INTRODUCTION

The ever-improving quality of seismic data has drawn attention to the importance of small-scale (wavelength to sub-wavelength) seismic heterogeneities in the crust, and has raised questions as to the validity of layered earth models. *A priori* constraints on the nature of small-scale seismic heterogeneities are useful for the planning of seismic experiments as well as for the interpretation, processing, and inversion of upper-crustal seismic data. Information on the statistical distribution of seismic velocities within the crust and lithosphere can be obtained from the inversion of scattered seismic waves (e.g. Wu & Aki 1985), or from a stochastic analysis of pertinent geological cross-sections and corresponding petrophysical data (e.g. Hurich & Smithson 1987; Holliger & Levander 1994a,b; Levander *et al.* 1994).

Borehole sonic-log data provide an opportunity to examine the nature of the small-scale seismic heterogeneity of the uppermost crust (Levander *et al.* 1994; Wu, Xu & Li 1994; Holliger, Green & Juhlin 1996). Sonic-log velocities are determined by measuring the time seismic waves take to travel between an ultrasonic source and one or more receivers. Source frequencies typically lie between 10 and 50 kHz (corresponding to wavelengths of about 0.10 to 0.60 m in crystalline rocks), source–receiver spacings range from about 1 to 3 m, and measurements are taken every 0.1 to 0.3 m along the borehole. The accuracy of a *P*-wave traveltime measurement is typically of the order of 1 per cent (Serra 1984). Sonic-log data thus represent 1-D, *in situ* measurements of seismic velocities with a resolution that is at least one order of magnitude higher than estimates obtained from the inversion of surface seismic data or from geological/petrophysical studies. The high resolution

of sonic-log data is of particular interest in view of the increasing importance of high-resolution seismic reflection and tomographic imaging of the upper crystalline crust (e.g. Milkereit *et al.* 1994; White *et al.* 1994).

For several decades sonic-log measurements have been performed routinely on sedimentary rocks for hydrocarbon exploration purposes. Applications of sonic-log data include the 'ground-truthing' of coincident or nearby seismic data, the calibration of stacking-, VSP-, and migration-velocity estimates, and, most importantly, estimation of porosities (e.g. Telford, Geldart & Sheriff 1990). For sedimentary environments, it is generally assumed that much of the local variability observed in sonic logs is due to primary or secondary porosity, level of saturation and the nature of the fluids filling the pores (e.g. Wyllie, Gregory & Gardener 1956; Telford *et al.* 1990). During the last decade, there has been a significant increase in the number of sonic logs measured in crystalline rocks for scientific and mineral exploration purposes. The most common application of sonic logs from crystalline terranes is the calibration of nearby seismic reflection and VSP data (Milkereit *et al.* 1994; White *et al.* 1994). These sonic logs show a level of small-scale variability that is similar to that of their sedimentary counterparts. However, the physical processes associated with these variations are not as well understood for crystalline rocks as they are for sedimentary environments.

The local variability of sonic-log velocities can be described

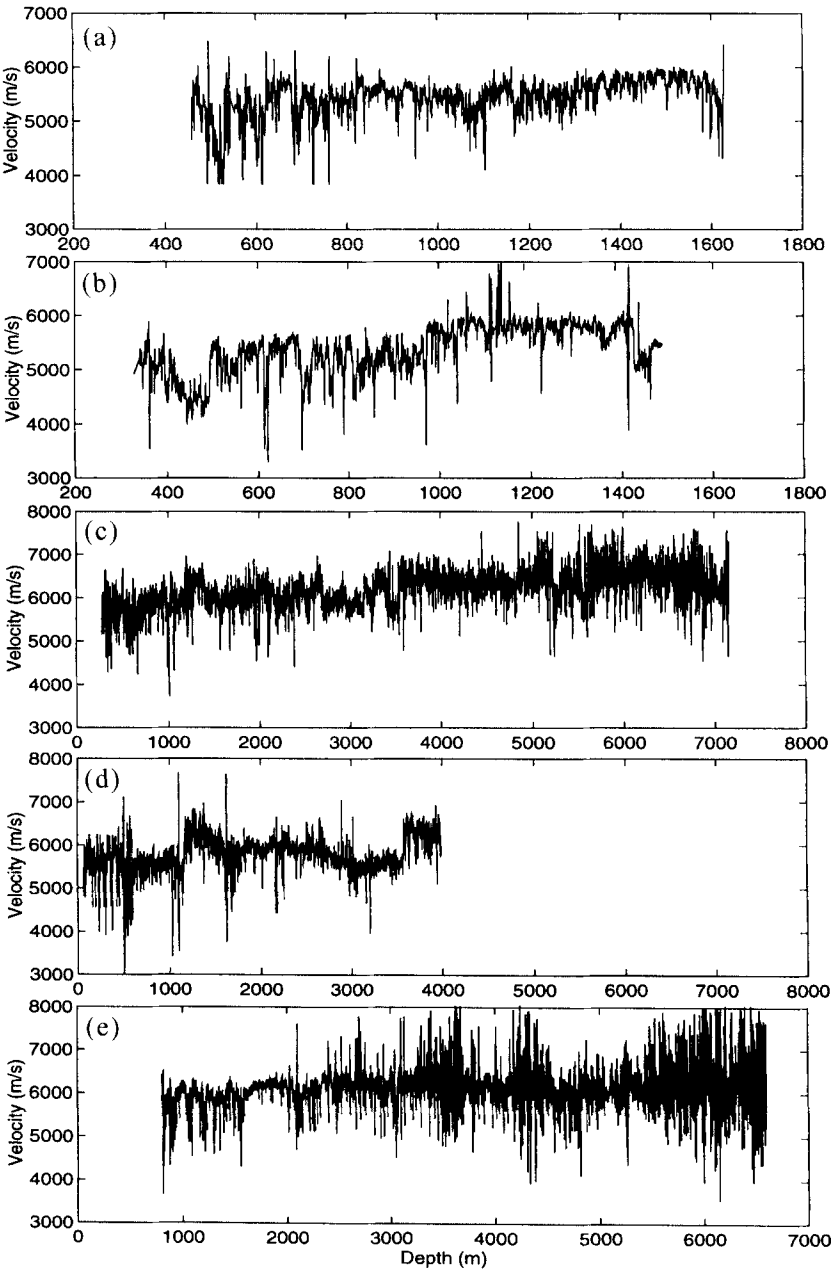

Figure 1. Raw sonic-log data considered in this study: (a) Leuggern (northern Switzerland), (b) Böttstein (northern Switzerland), (c) KTB-1 (south-eastern Germany), (d) KTB-2 (south-eastern Germany), (e) Stenberg-1 (Siljan Ring, Sweden), (f) Sudbury-1 (Sudbury structure, Canada), (g) Sudbury-2 (Sudbury structure, Canada), (h) Abitibi-1 (Abitibi Greenstone Belt, Canada), (i) Abitibi-2 (Abitibi Greenstone Belt, Canada), (j) Cajon Pass (California, USA). Note the different scales of the plots.

using a statistical approach. Resulting stochastic models of seismic heterogeneity are useful for characterizing seismic scattering in the upper crust, predicting attenuation and phase fluctuations, quantifying stratigraphic filtering effects, and optimizing deconvolution and inversion operators (Frankel & Clayton 1986; Todoeschuck & Jensen 1988; Pilkington & Todoeschuck 1991). Most of the research in this field has been conducted on sonic logs from sedimentary environments (Walden & Hosken 1985). In a previous paper, I presented a stochastic analysis method for upper-crustal sonic-log data (Holliger *et al.* 1996). In an attempt to place constraints on the origin of the small-scale variability of sonic-log velocities, this method is applied here to a wide variety of *P*-wave sonic-log data from the upper crystalline crust.

DATA BASE

This section gives a brief description of the sonic-log data analysed in this study (Fig. 1).

Switzerland: Leuggern and Böttstein

The Leuggern (Fig. 1a) and Böttstein (Fig. 1b) holes are located some 2 km apart and were drilled by Nagra (Swiss National Cooperative for the Disposal of Radioactive Waste) as part of a project to investigate the physical properties of the Variscan basement in the northern foreland of the Alps (Thury *et al.* 1994). Both holes are approximately 1500 m deep and penetrate 200 to 400 m of Mesozoic sediments before reaching the

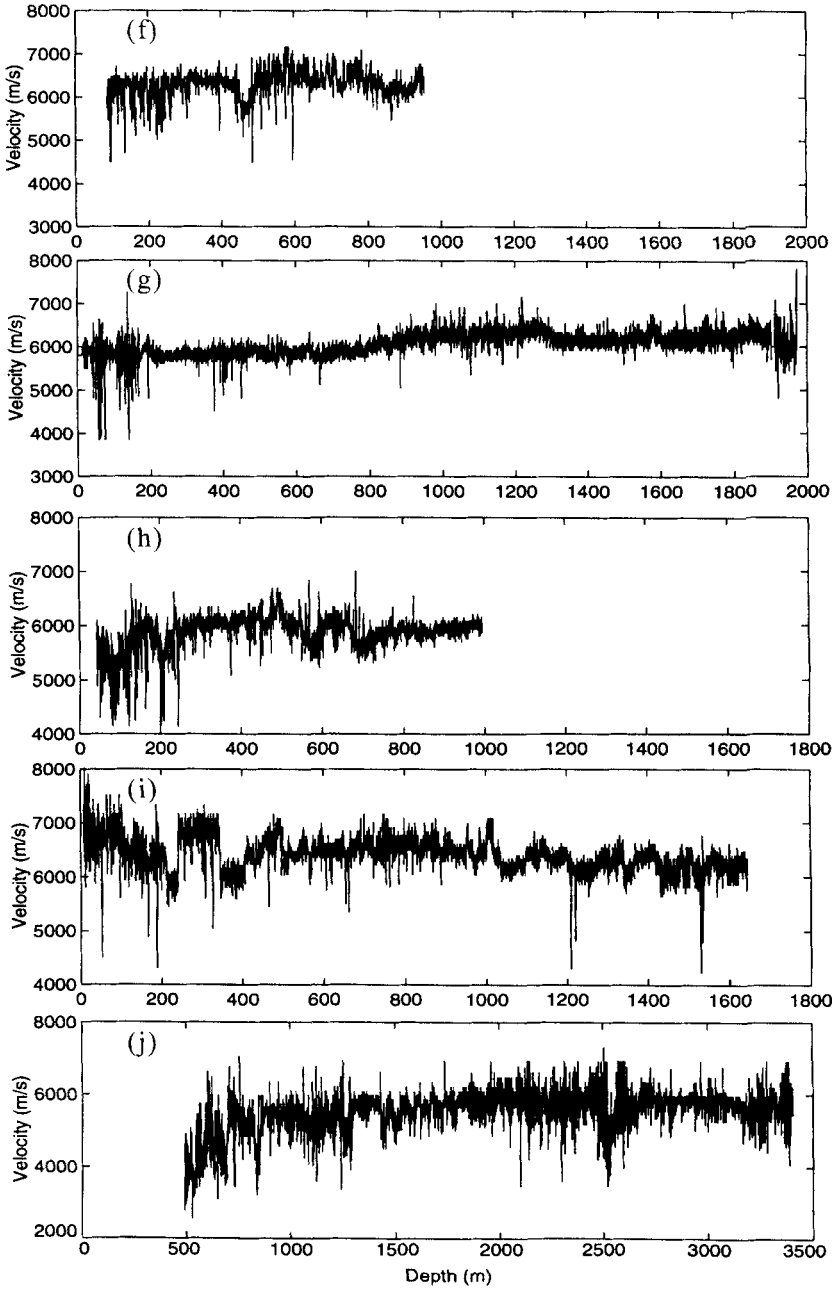

Figure 1. *(Continued.)*

crystalline basement. Lithologies along the basement section of the Leuggern borehole are amphibolite-facies paragneisses to a depth of 1380 m, followed by granitic rocks to the base of the hole at 1690 m. The sedimentary protoliths of the paragneisses were deposited during the Late Proterozoic and were subsequently multiply deformed and metamorphosed. The basement section of the Böttstein hole consists entirely of granitic rocks. Radiometric dating indicates early Carboniferous ages, both for the intrusion of the granitic rocks and for the amphibolite-facies metamorphism of the paragneisses. The sonic data were acquired at 0.152 m intervals using a compensated sonic tool (see e.g. Telford *et al.* 1990) with a minimum source–receiver spacing of about 1.0 m.

Germany: KTB-1 (main hole) and KTB-2 (pilot hole)

The two boreholes at the German deep drill site are only 200 m apart and reach depths of approximately 9000 (KTB-1; Fig. 1c) and 4000 m (KTB-2; Fig. 1d). Here sonic-log data for KTB-1 are considered to a depth of about 7200 m. The scientific objectives of this deep continental drilling project were to investigate the structure and composition of the Variscan upper crust and to explore the origins of seismic reflections from the crystalline crust. Both boreholes penetrate amphibolite-facies paragneisses interlayered with metabasites (Franke 1989). Radiometric age dating suggests an early to middle Variscan peak of metamorphism for the paragneisses and mafic rocks (Hansen, Teufel & Ahrendt 1989). The sonic-log data are sampled at 0.152 m intervals. The uppermost 4000 m of both boreholes were logged with a sonic array tool. For the remaining part of KTB-1, a sonic shear tool was used. Both tools have minimum source–receiver spacings of about 1.0 m (X.-P. Li, personal communication 1994).

Central Sweden: Stenberg-1

The Stenberg-1 borehole (Fig. 1e) is located in Precambrian rocks of the Siljan Ring impact structure. It was drilled for the exploration of abiogenic gas flux through the crystalline basement. The hole mostly penetrates granitic rocks containing intrusions of doleritic dykes and sills (Juhlin 1990). These granites and dolerites were intruded at various times during the Proterozoic, whereas the impact event occurred during the Devonian. Sonic-log data are available from 770 to 6569 m depth and are sampled at 0.304 m intervals. The data were acquired using a sonic array tool with an approximate minimum source–receiver spacing of 1.0 m (C. Juhlin, personal communication 1994).

Canada: Sudbury impact structure

Located along the north rim of the Sudbury structure, the Sudbury-1 (Fig. 1f) and Sudbury-2 (Fig. 1g) boreholes reach depths of about 900 and 2000 m, respectively (Milkereit *et al.* 1994; White *et al.* 1994). Both boreholes were drilled for mineral exploration purposes. The Sudbury structure was formed as a result of an early Proterozoic impact event and consists of layered mafic intrusive rocks and impact breccia. The boreholes were logged at 0.1 m intervals using an uncompensated sonic tool with a minimum source–receiver spacing of about 1.0 m (B. Milkereit, personal communication 1994).

Canada: Abitibi Greenstone Belt

The Abitibi Greenstone Belt is located in the Archean Superior Province and consists of volcanic–plutonic arc sequences that were accreted to the Superior craton when it stabilized 2600 to 2800 Ma ago. The two boreholes considered here were drilled for mineral exploration purposes. They are referred to as Abitibi-1 (Fig. 1h) and Abitibi-2 (Fig. 1i) and reach depths of about 900 and 1700 m, respectively. Abitibi-1 penetrates andesites, rhyolites, and gabbros. Lithologies encountered along the Abitibi-2 borehole are andesites, rhyolites, tonalites, and tuffs (B. Milkereit, personal communication 1995). Both boreholes were logged at 0.1 m intervals using an uncompensated sonic tool with a minimum source–receiver spacing of about 1.0 m (B. Milkereit, personal communication 1995).

USA: Cajon Pass

The Cajon Pass borehole (Fig. 1j) is located 32 km north of San Bernardino, California, 4 km from the San Andreas fault (see special editions of Geophysical Research Letters, vol. 15, pp. 931 ff., 1988; Journal of Geophysical Research, vol. 97, pp. 4991 ff., 1992). The borehole is 3500 m deep and penetrates 490 m of late Mesozoic to Neogene clastic sediments before entering the crystalline basement. Penetrated basement consists of various gneissic and granitic rocks of Precambrian to Mesozoic age (Silver & James 1988). Lithological contacts within the basement section seem to be mostly associated with larger shear zones. The first 400 m of the crystalline basement consists of pervasively sheared and deformed crystalline rocks. The borehole was logged at 0.152 m intervals using a compensated sonic tool with a minimum source–receiver spacing of about 1.0 m (P. Leary, personal communication 1995).

SEPARATION OF STOCHASTIC AND DETERMINISTIC COMPONENTS

Eqs (A1) to (A5) in the Appendix provide the information required to invert the observed sonic-log data for the second-order statistics of the small-scale *in situ* velocity fluctuations (Goff & Jordan 1988; Holliger *et al.* 1996). To do this, the stochastic and deterministic components of the observed sonic-log velocities must first be separated. It has to be pointed out that, although the removal of large-scale trends is a common practice in statistics (e.g. Chatfield 1980), there are no clear rules or systematic guidelines as to how this separation of deterministic and stochastic components should be performed. In particular, there are conflicting points of view as to the maximum frequency that should be contained in the deterministic component.

From a purely statistical point of view, a possible objective of trend removal is to make the residual stochastic process stationary. This may be achieved by subtracting trends containing significant high-frequency information, for example by differencing the observed data sequence, which is equivalent to subtracting a two-point running mean (e.g. Chatfield 1980). For many applications, this practice is questionable because the residual data sequence is likely to be dominated by uncorrelated noise, and because the trend itself is so variable that its classification as deterministic may be inappropriate. From a seismological point of view, it is natural to associate the stochastic and deterministic parts of crustal velocity struc-

ture with the scattered and specular parts, respectively, of seismic wavefields. Based on this classification, the deterministic trend primarily depends on the dominant frequency, or wavelength, of the seismic signal considered. Although the transition from scattering to specular wave propagation is not sharp, it is generally expected to occur for $\alpha/\lambda \gg 1$, i.e. for heterogeneity scales α that are significantly (at least 5 to 10 times) larger than the dominant wavelengths λ of the seismic signal considered (Wu & Aki 1988). It should be understood that α is independent of the correlation length a used to characterize random media (see Appendix). For an average upper-crustal velocity of 6000 m s^{-1} the minimum wavelength α of the deterministic trend thus lies at about 3000 m for a dominant frequency of 10 Hz (local earthquake and crustal wide-angle seismic data), at about 1000 m for a dominant frequency of 30 Hz (deep crustal reflection seismic data), and at about 300 m for a dominant frequency of 100 Hz (high-resolution reflection seismic data).

With reference to low-to-intermediate seismic frequencies (< 50 Hz) the deterministic trend may therefore be approximated by a low-order polynomial best fit of the sonic-log data. The order of the polynomial should increase with the length of the sonic log and/or the frequency of the seismic data considered. From a methodological point of view, this approach agrees with the one proposed by Bendat & Piersol (1986), who recommend fitting a low-order polynomial to the observed data. They point out that the chosen trend should be physically reasonable and clearly apparent in the original data. From a phenomenological point of view, this is consistent with results of seismic wide-angle experiments (Mueller 1977) and laboratory measurements (Christensen 1979; Burlini & Fountain 1993), both of which suggest a quasi-linear increase of the large-scale upper-crustal velocity–depth function.

In the following, the effects of removing trends containing progressively higher maximum frequencies from the data are investigated, and the Leuggern (short sonic log) and KTB-1 (long sonic log) data sets are used to illustrate interpretation concepts and results. After analysing all available sonic logs, these two data sets were found to be representative of the data base considered.

ANALYSIS ASSUMING LOW-ORDER POLYNOMIAL DETERMINISTIC TRENDS

For all data sets of this study, the slopes of the best-fitting (in a least-squares sense) linear trends were compatible with results from wide-angle seismic data (Mueller 1977) and laboratory experiments (Christensen 1979; Burlini & Fountain 1993). After removing such a linear trend, the residual sonic-log velocity fluctuations could be characterized reasonably well by Gaussian probability distributions (Fig. 2). As is evident in Fig. 2, the most significant deviations from the corresponding best-fitting Gaussian probability density functions are the extended negative tails, i.e. low velocities. The fact that a Gaussian-type distribution is characteristic of both short (< 1000 m) and long (> 7000 m) sonic logs suggests that it reflects an intrinsic statistical property of the upper-crustal seismic fabric and is not simply a consequence of the central limit theorem (Bendat & Piersol 1986).

Inverting the residual stochastic process yields the parameters defining the autocovariance function of the *in situ* velocity variations along the borehole (Table 1). The inversion algorithm

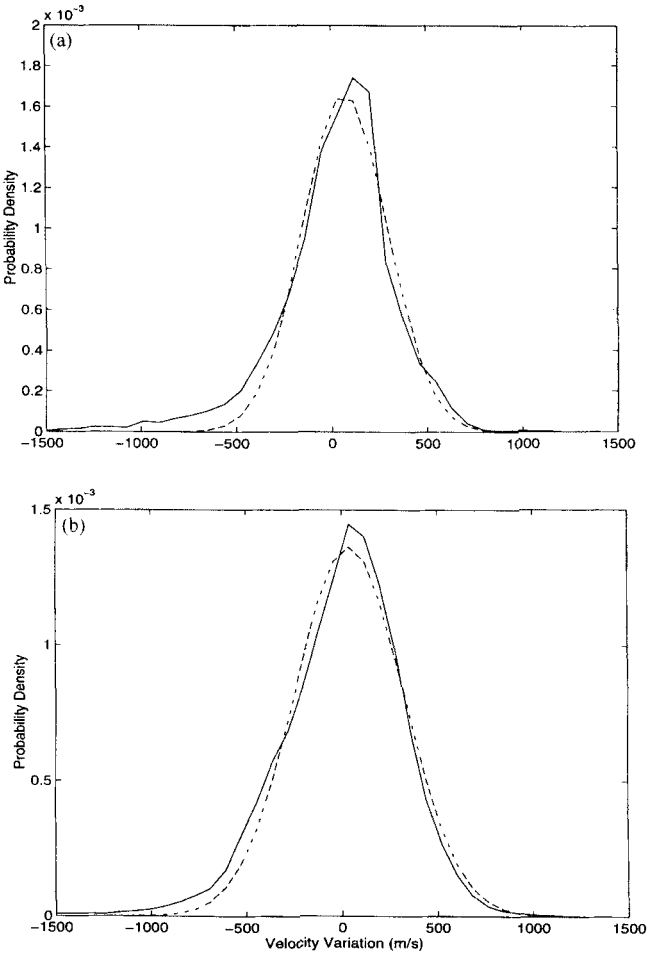

Figure 2. Probability density functions of (a) Leuggern and (b) KTB-1 data after removing a linear trend defined by a corresponding least-squares best fit through the original data. Solid lines: probability density functions of observed data; dashed lines: best-fitting Gaussian probability density functions.

used is essentially identical to that developed by Goff & Jordan (1988) for bathymetric data. Starting values for the Hurst numbers and correlation lengths were derived from the slopes of the power spectra (see eq. A6; Wu *et al.* 1994) and from the first zero-crossings of the autocovariance functions (Goff & Jordan 1988), respectively. The autocovariance functions of the residual sonic-log velocities are shown in Fig. 3, together with their best-fitting (in a least-squares sense) model autocovariance functions. In all cases the data model described in the Appendix provided a good-to-excellent match to the autocovariance functions of the residual sonic-log fluctuations.

Despite the different geological settings of the individual boreholes and different noise levels of the sonic logs, the results are surprisingly uniform: low Hurst numbers of between 0.09 and 0.18, short to intermediate correlation lengths of 60 to 160 m, and standard deviations (defined as the square root of the variance) of 170 to 400 m s^{-1} (Table 1). The uncertainties of the Hurst numbers and correlation lengths are estimated to be 20 per cent or less, i.e. Hurst numbers and correlation lengths differing by more than 20 per cent from the values listed in Table 1 lead to an unacceptable match between the observed and modelled autocovariance functions. These error estimates are based on the diagonal elements of the parameter covariance matrix.

Table 1.

Borehole	ν	a (m)	σ_h (m/s)	σ_n (m/s)
Leuggern	0.14	60	317	66
Böttstein	0.12	80	370	71
KTB-1	0.10	160	315	72
KTB-2	0.13	150	358	75
Stenberg-1	0.09	160	300	253
Sudbury-1	0.11	70	282	96
Sudbury-2	0.10	150	169	123
Abitibi-1	0.18	110	266	111
Abitibi-2	0.18	60	241	118
Cajon Pass	0.11	140	399	171

ν: Hurst number; a: correlation length; σ_h: standard deviation of *in situ* velocity fluctuations; σ_n: standard deviation of white noise present in the sonic log data.

Table 2.

Borehole/Trend	ν	a (m)	σ_h (m/s)	σ_n (m/s)
KTB-1				
linear trend	0.10	160	315	72
second-order polynomial	0.10	130	309	72
third-order polynomial	0.10	120	308	72
300 m running-mean	0.10	45	247	72
KTB-2				
linear trend	0.13	150	358	75
second-order polynomial	0.13	150	349	75
third-order polynomial	0.13	140	341	75
300 m running-mean	0.13	55	271	75
Stenberg-1				
linear trend	0.09	160	300	253
second-order polynomial	0.09	140	292	253
third-order polynomial	0.09	120	289	253
300 m running-mean	0.09	40	248	253
Cajon Pass				
linear trend	0.11	140	399	171
second-order polynomial	0.11	90	383	171
third-order polynomial	0.11	85	368	171
300 m running-mean	0.11	40	304	171

There is a certain trade-off between Hurst number, correlation length, and the system filter, yet I found it impossible to compensate significantly larger Hurst numbers with correspondingly shorter correlation scales, even when ignoring the filtering effects of the logging tool (Fig. 4). Moreover, in all cases considered, the low Hurst numbers inferred are also consistent with the average slopes of sonic-log power spectra (Wu *et al.* 1994; Sato & Shiomi 1995; H. Sato, personal communication 1995).

Comparable results were obtained when removing quadratic and cubic polynomials, defined by least-squares best fits through the sonic-log data, from the KTB, Stenberg-1, and Cajon Pass sonic logs (Table 2). Although shorter correlation lengths (Fig. 5) and smaller standard deviations of the velocity

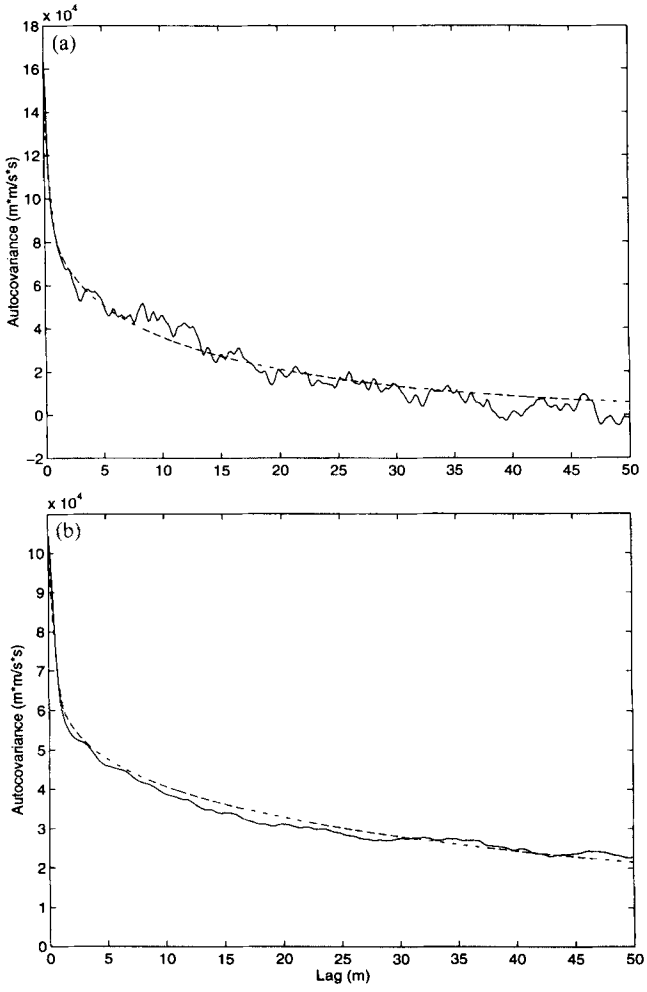

Figure 3. Autocovariance functions of (a) Leuggern and (b) KTB-1 sonic-log data after removing a best-fitting linear trend. Solid lines: autocovariance functions of observed data; dashed lines: best-fitting von Kármán autocovariance functions.

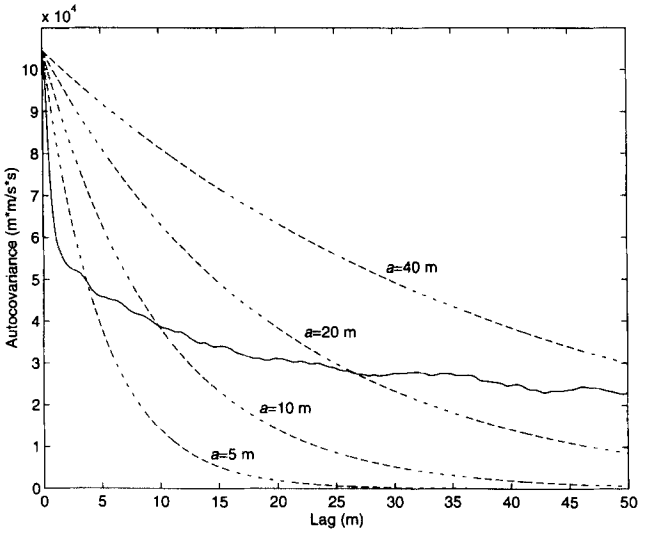

Figure 4. Solid line: autocovariance function of KTB-1 data; dashed lines: exponential autocovariance functions (Hurst number $\nu = 0.5$) for a variety of correlation lengths ($a = 5$, 10, 20 and 40 m). No corrections for system response and noise have been applied.

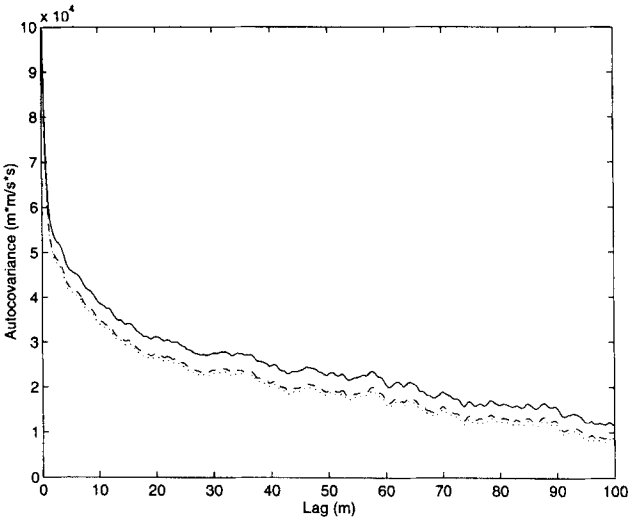

Figure 5. Autocovariance functions of KTB-1 data after removing different polynomial trends defined by corresponding least-squares best fits through the original sonic-log data. Solid line: linear trend; dashed line: quadratic trend; dotted line: cubic trend.

fluctuations are observed after subtracting such higher-order polynomials, the results are quite similar to those obtained for a linear trend (Table 2). In particular, the Hurst numbers and the standard deviations of the white system noise do not seem to be affected by the order of the polynomial defining the trend.

ANALYSIS ASSUMING HIGHER-FREQUENCY DETERMINISTIC TRENDS

The estimation of seismic heterogeneity relevant to the scattering of higher-frequency (> 100 Hz) seismic data requires the removal of all spectral components with wavelengths longer than a given threshold from the sonic-log data. For the longer sonic logs considered here, this has been achieved by removing a running mean with a window length of $\alpha = 300$ m (see above). Fig. 6 illustrates this trend for the KTB-1 data. The removal of such a trend notably reduces the standard deviation and the correlation length of the velocity fluctuations but again does not affect the Hurst number and the standard deviation of the white noise (Fig. 7; Table 2).

An interesting observation is that the correlation length estimates seem to be even more consistent between the different data sets than was the case after removing low-order polynomials. This may be due to the fact that the largest wavenumber k_{filter} contained in the trend is larger than the corner wavenumber of the power spectrum of the stochastic process, which is defined by $k_{\text{corner}} = 1/a$ (see Appendix). The removal of such a high-frequency trend is equivalent to applying a high-pass filter, and results in a modified band-limited power-law process $[(1 + k^2 a_{\text{filter}}^2)^{-\beta/2}$-decay of the power spectrum] whose correlation length a_{filter} is determined by the upper cut-off wavenumber of the filter k_{filter}. For a 300 m running-mean filter, the reciprocal value of the cut-off wavenumber is $a_{\text{filter}} = 1/k_{\text{filter}} = 300/2\pi \approx 48$ m, which is in fact quite close to the corresponding estimates of the correlation lengths shown in Table 2.

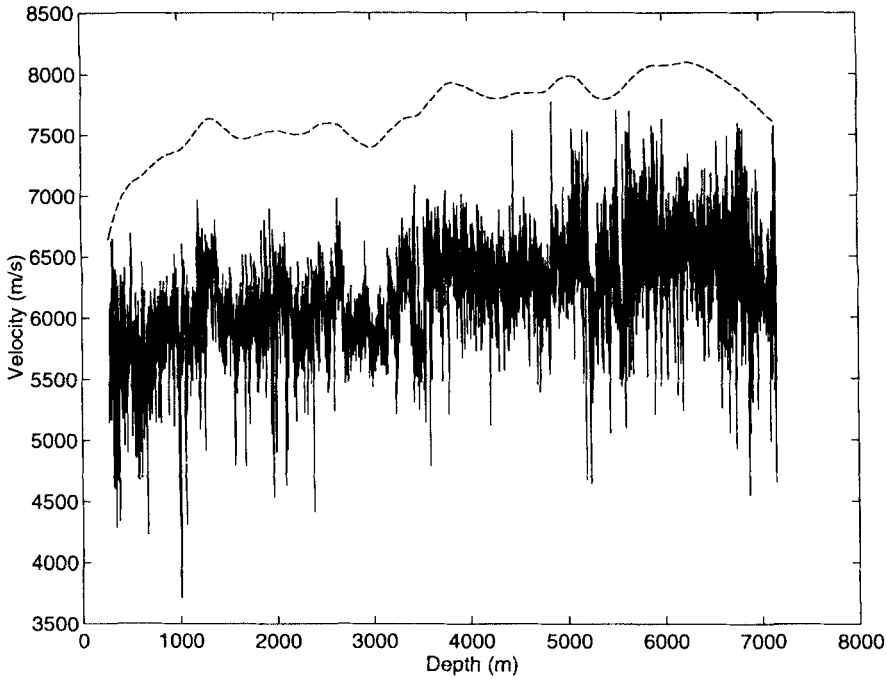

Figure 6. Running mean with a window length of 300 m of KTB-1 sonic-log data (dashed line) together with the original data. The trend defined by this running mean has been shifted by $+1500\ \mathrm{m\ s^{-1}}$ for clarity.

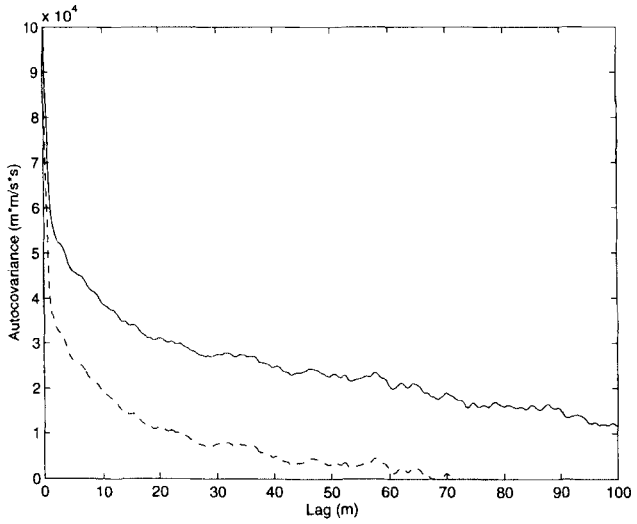

Figure 7. Autocovariance functions of KTB-1 sonic-log data after removing a linear trend (solid line) and a 300 m running-mean trend (dashed line).

STATISTICAL UNIFORMITY

For the longer sonic logs in the considered data base it is important to know how representative the global stochastic estimates (Table 1) are for smaller subsets of the sonic logs. For this purpose the linearly trend-corrected KTB-1 log has been subdivided into five 1375 m long subsets. The length of such a subset is thus comparable to that of the shorter sonic logs analysed in this study. These subsets have been analysed separately, and the results are shown in Table 3. The largest discrepancies between the local and global estimates of the Hurst numbers and correlation lengths are about 30 per cent. Given that the inherent uncertainty of the inversion process lies in the same range, it is argued that, although the strict criteria of statistical stationarity may not be fulfilled, the stochastic nature of the KTB-1 sonic-log fluctuations is relatively uniform over the entire length of the log and largely independent of the lithological sequence penetrated. Similar results were obtained for the KTB-2 and Cajon Pass logs. The subsets of the Stenberg-1 log show a larger internal variability, which seems to reflect variations in data quality (Holliger *et al.* 1996). Overall, these results are consistent with those of Li & Haury

Table 3.

Data	Depth (m)	ν	a (m)	σ_h (m/s)	σ_n (m/s)
Full log	285-7160	0.10	160	315	72
Subset 1	285-1660	0.11	170	342	57
Subset 2	1660-3035	0.09	130	256	50
Subset 3	3035-4410	0.12	205	292	50
Subset 4	4410-5785	0.09	150	308	90
Subset 5	5785-7160	0.08	170	357	97

(1995), who used the wavelet transform to calculate local variations in the slope of the power spectrum of the KTB data. Their results indicate that the fluctuations are small and centred around a relatively uniform global average, which is consistent with the results of Table 3.

COMPARISON WITH SYNTHETIC DATA

To assess the importance of non-Gaussian components in the sonic-log fluctuations, synthetic realizations with corresponding stochastic parameters (Table 1) and Gaussian probability density functions were generated. These synthetic data were created by employing the following procedure: (1) filter a uniformly distributed random number sequence with the square root of the power spectrum of the considered stochastic process; (2) take the inverse Fourier transform; (3) filter the resulting stochastic process with the estimated system filter of the sonic tool and scale with respect to the standard deviation of the *in situ* velocity fluctuations; and (4) add the estimated amount of white noise. The resulting synthetic sonic-log variations are shown in Fig. 8, together with the observed sonic-log data. As expected, because of the good match between the modelled and observed autocovariance functions (Fig. 3), the synthetic stochastic sonic logs compare well with the real ones, apart from lacking the negative outliers and being somewhat too uniform. The presence of negative outliers in the observed data and the more uniform nature of the synthetic data are both indicative of higher-order (>2) statistical moments, i.e.

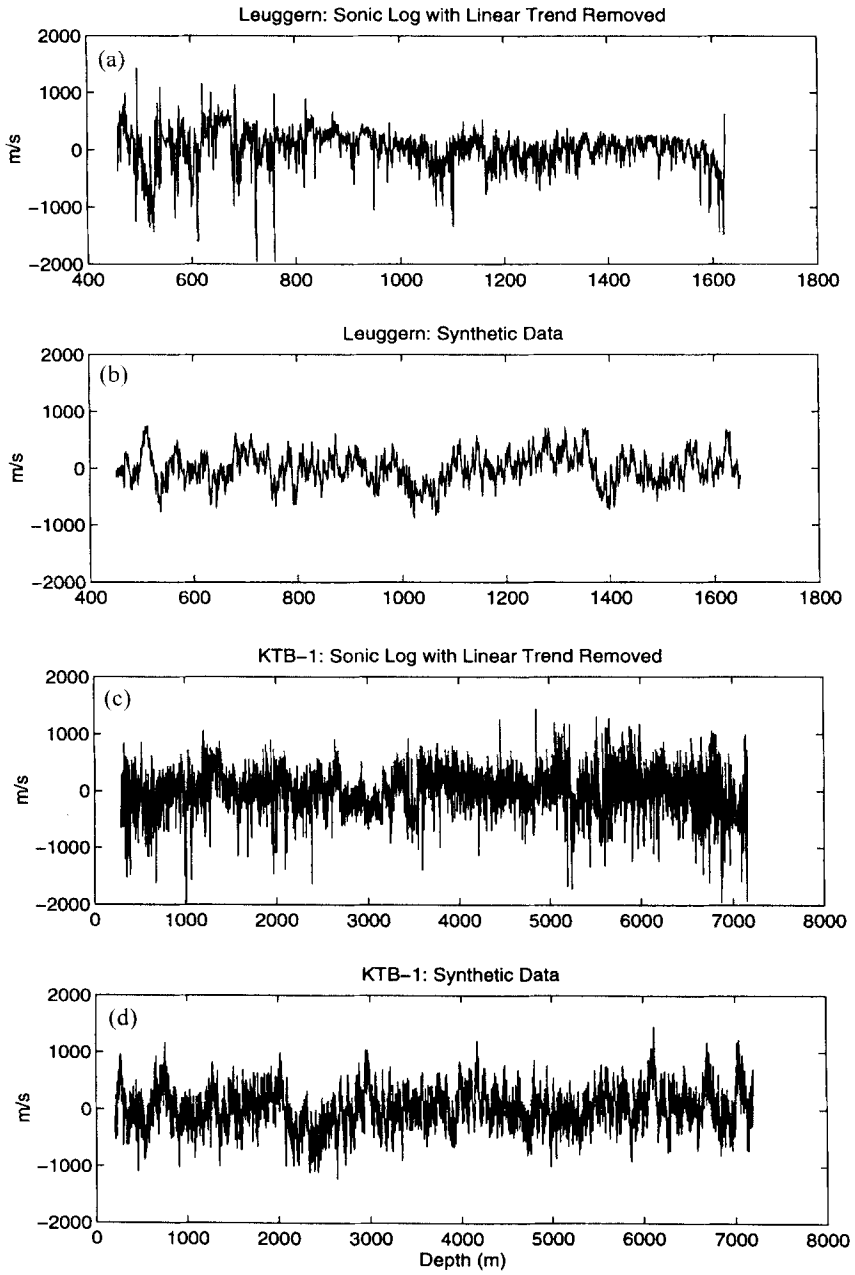

Figure 8. Comparison of the observed sonic-log variations after subtracting a linear deterministic trend with corresponding synthetic data. (a) Observed Leuggern data; (b) synthetic Leuggern data; (c) observed KTB-1 data; (d) synthetic KTB-1 data.

deviations from ideal Gaussian probability density functions, which are not included in this analysis.

COMPARISON WITH OTHER ESTIMATES OF CRUSTAL SEISMIC HETEROGENEITY

Estimates from borehole data

Levander *et al.* (1994) have analysed a short (~350 m long) sonic log from the Cornubian granite in south-western England, and have inferred a von Kármán autocovariance function with a Hurst number of 0.20–0.25 and a correlation length of 10 to 20 m. They speculate that this correlation length may correspond to the spacing of joint sets along the borehole. These estimates are comparable to the results summarized by Wu & Aki (1988) for similarly short logs.

The results for the two KTB boreholes can be compared directly to those of recent studies by Wu *et al.* (1994) and Kneib (1995). Wu *et al.* (1994) subtracted linear trends from the KTB-1 and KTB-2 *P*-wave sonic logs and then used the slope of the power spectra to estimate the Hurst numbers. Their estimates of the Hurst numbers agree very well with those given in Table 1. After plotting the power spectrum in double-logarithmic format, a change in slope is expected to occur near $ka \approx 1$ for band-limited self-affine data (see eq. A6). However, Wu *et al.* (1994) found no evidence of a change in slope at intermediate to low wavenumbers, and therefore argued that self-affine behaviour extends unchanged from very short wavelengths of a few metres to a maximum wavelength of at least 1000 m. This conclusion is not supported when modelling the observed autocovariance functions as von Kármán-type functions, which are the time-domain expressions of the type of power spectrum used by Wu *et al.* (1994). The discrepancy may be due to the typically large fluctuations of the power spectrum, to its relatively slow decay (characteristic of low Hurst numbers), and/or to the inherently low resolution of the double-logarithmic scale, all of which tend to obscure changes in slope. To illustrate this, the power spectra of both the observed and synthetic KTB-1 data (Figs 8c and 8d) are shown in Fig. 9. In neither case is a change in slope in the low-wavenumber range obvious.

Kneib (1995) analysed the sonic (*P*- and *S*-wave) and density data of the KTB main hole. He computed local estimates of the autocovariance function in 244 m long data windows after subtracting the local mean value. The individual data windows overlapped by 122 m. The resulting local autocovariance functions were stacked in order to obtain a high-pass filtered estimate of the autocovariance function of the entire sonic log. This global estimate of the autocovariance function was then modelled by superposing two exponential autocovariance functions with correlation lengths of 1 and 20 m. This stochastic analysis approach explicitly excludes any wavelengths longer than 244 m. As outlined above, applying such a high-pass filter to a power-law process, i.e. $k^{-\beta}$-decay of the power spectrum in the relevant wavenumber range, is expected to produce a correlation length of the order of 40 m. Moreover, superposition of several exponential stochastic processes (Hurst number $\nu = 0.5$) produces an ensemble process dominated by a Hurst number close to zero and a correlation length corresponding to about 1–2 times the largest correlation length present in the superposed exponential processes (here 20 m); at scales smaller than the shortest correlation length (here 1 m), the resulting ensemble process is dominated by exponential behaviour (Walden & Hosken 1985). Fig. 10 demonstrates that Kneib's (1995) ensemble process is in fact well approximated by a von Kármán function with a Hurst number of 0.13 and a correlation length of 30 m, and that exponential behaviour at short lags is consistent with the low-pass filtering effects of the logging process. In summary, although not immediately apparent because of the combination of several exponential autocovariance functions, Kneib's (1995) results are fully consistent with the findings of this study.

Leary (1991) used the 'rescaled-range technique' (Mandelbrot 1983) to analyse the Cajon Pass sonic-log data from 2000 to 3500 m depth. He inferred a Hurst number of 0.7 and scale independence from 1.5 to at least 1500 m. This technique is based on the cumulative sums of parts of the observed data sequence, and thus emphasizes large-scale trends rather than small-scale local fluctuations. As in the case of power spectra, the analysis is carried out in the double-logarithmic domain. Neither the inferred Hurst number nor the scale range is compatible with the results obtained here, and these parameters (Hurst number 0.7; correlation scale >1500 m) do not allow for the generation of synthetic data sets that bear any close resemblance to the observed sonic-log data (Fig. 11). This finding is in agreement with the findings of North & Halliwell (1994), who showed that Hurst number estimates by the rescaled-range technique tend to be biased towards values that are significantly too high.

Stochastic analysis of geological cross-sections and petrophysical data

Detailed geological cross-sections of pertinent parts of the Earth's crust have been converted to stochastic seismic velocity models (Holliger & Levander 1994a,b; Levander *et al.* 1994). Each mapped lithology is assigned a representative average velocity, and the statistical properties of the resulting seismic velocity models are examined in a fashion similar to that described in the Appendix of this paper. So far, this technique has been applied to the Phanerozoic middle- and lower-crustal sections exposed in the Ivrea and Strona–Ceneri zones (northern Italy) (Holliger & Levander 1994a, b), and to the Archean middle crust of the Lewisian gneiss complex (Scotland) (Levander *et al.* 1994). The resulting autocovariance functions were found to be well approximated by von Kármán functions, albeit with generally higher Hurst numbers (0.5–0.2) and more variable and generally longer correlation lengths (38–2600 m) than obtained here. Moreover, the inferred probability density functions are discrete (binary/ternary) rather than Gaussian. Differences between the results presented here and those of other studies can be explained by the inherently lower resolution of the geological maps analysed (10 to 100 m as opposed to 1 to 2 m for the sonic logs), and by the effective smoothing and binning of the seismic structure that occurs when each mapped lithology is assigned a single distinct velocity.

ORIGIN OF SMALL-SCALE VELOCITY VARIATIONS IN SONIC LOGS

Variability of crustal velocities evidenced by petrophysical studies

The results of this study show no clear relationship between the statistics of sonic-log velocities and the lithological sequences

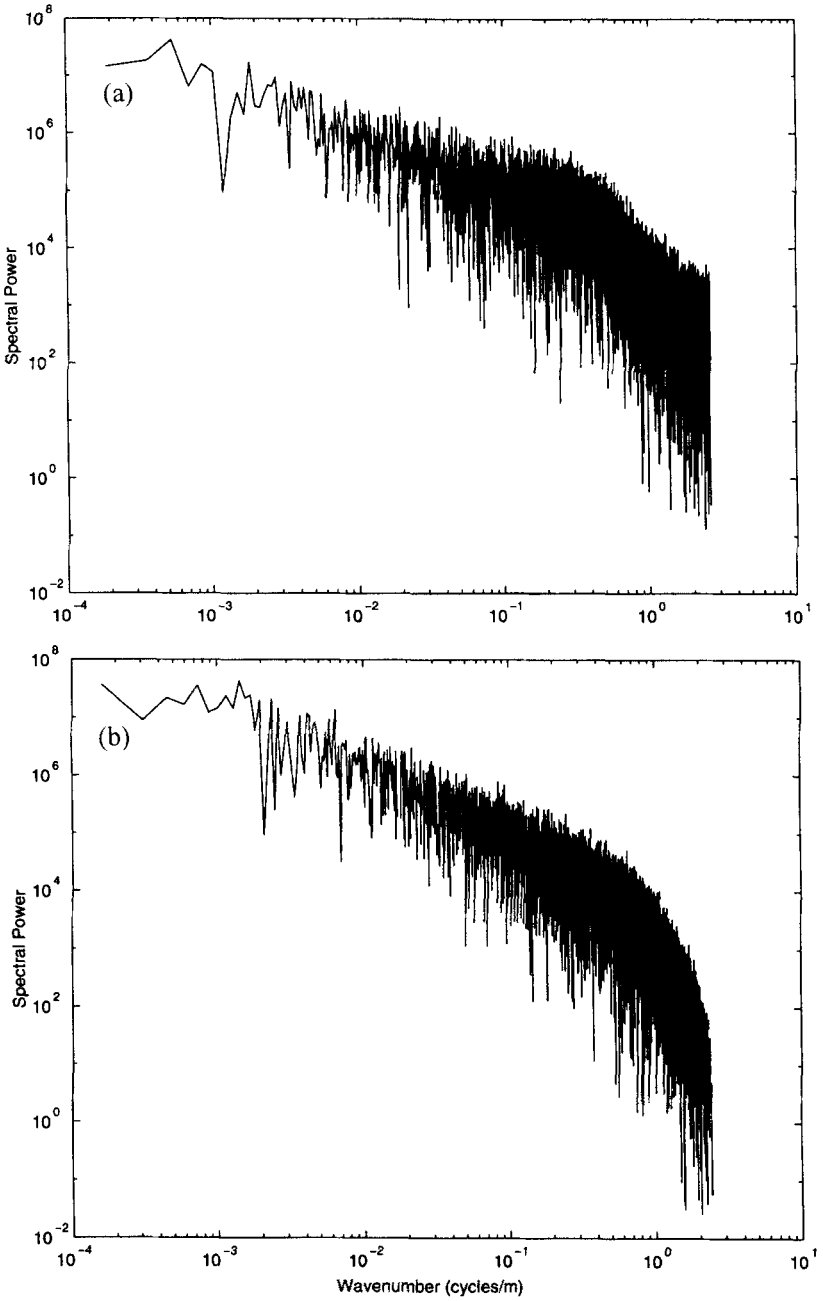

Figure 9. Power spectra of (a) observed KTB-1 data (Fig. 8c) and (b) corresponding synthetic data (Fig. 8d). A best-fitting linear trend has been subtracted from the observed data. The change in slope at high wavenumbers is due to inherent averaging of the logging process over the active length of the tool.

penetrated by the boreholes. For example, despite the approximately bimodal petrology of the lithologies (mafic amphibolites and intermediate-to-acid paragneisses) penetrated by the KTB boreholes, the corresponding sonic-log velocity variations have quasi-Gaussian distributions (Fig. 2; Wu *et al.* 1994). This could be due to the overlap of velocities for different rock types and to the variability of seismic velocity within the same lithological units (Christensen 1979).

Salisbury, Iuliucci & Long (1994) have analysed the seismic velocities of the various lithologies encountered in the two Sudbury boreholes. The average ultrasonic velocities of the different crystalline lithological units, measured in the laboratory at 600 MPa pressure and room temperature, ranged from 6100 to 6600 m s^{-1}, and the corresponding standard deviations from 130 to 250 m s^{-1}. These velocities and standard deviations compare reasonably well with those from the sonic logs (Milkereit *et al.* 1994; White *et al.* 1994). Burlini & Fountain (1993) analysed numerous gneissic rocks of similar composition from the exposed middle- and lower-crustal cross-section in the Ivrea and Strona-Ceneri zones in northern Italy. The average velocities of the ultrasonic *P*-wave velocities and their respective standard deviations, measured at 600 MPa pressure and room temperature, were 6400 ± 190 m s^{-1} for mid-crustal samples and 6790 ± 380 m s^{-1} for the lower-crustal samples. The variability of velocities within lithologically similar units documented by these investigations is comparable to

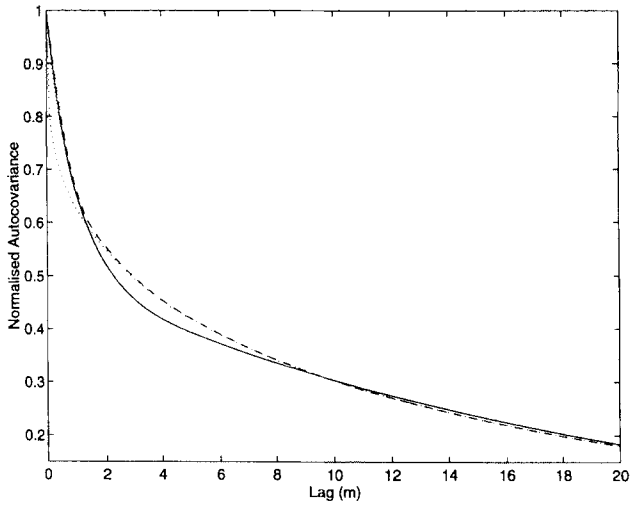

Figure 10. Solid line: autocovariance function resulting from the superposition of two exponential functions with correlation lengths of 1 and 20 m (Kneib 1995). Also shown is the best-fitting von Kármán autocovariance function with a correlation length of 30 m and a Hurst number of 0.13 with (dashed line) and without (dotted line) consideration of system response. System filter $f(z)$ is a running mean with a window length of 1.0 m, which corresponds approximately to the minimum source–receiver spacing of the sonic tools used to acquire the KTB data. All autocovariance functions are normalized.

that found in sonic logs considered in this work. Since the above measurements were made at high confining pressures, corresponding approximately to lithostatic pressure at 18 km depth, it is generally assumed that microcracks are largely closed and that the observed velocity variability primarily reflects chemical and/or microstructural variability between the individual samples.

Variability of upper-crustal velocities due to fracturing

Fractures of all scales are ubiquitous in the upper crystalline crust, and their statistical distribution follows self-affine scaling laws that appear to be independent of geological age, lithological composition, tectonic setting, and depth (Scholz *et al.* 1993). Paillet & White (1982) modelled the sonic-log response of fractured media. They found that sonic transit times, and thus sonic-log velocities, are heavily dependent on both micro- and macrofractures. This theoretical result has been supported by Moos & Zoback (1983), who compared the distribution of macrofractures with sonic-log velocities in several boreholes penetrating the upper crystalline crust. For the Cajon Pass borehole, Leary (1991) found a significant correlation between sonic and resistivity logs, but no comparable correlation of these log data with the natural gamma logs. Since natural gamma logs are primarily sensitive to the petrology of the penetrated lithologies, Leary (1991) argued that sonic and resistivity logs are likely to be dominated by the effects of fracturing.

In order to explain the surprisingly uniform *S*-wave anisotropy found in various types of upper crust, Crampin (1994) proposed the concept of 'fracture criticality'. According to this model, the range of crack densities between the extreme, and rarely observed, cases of totally intact and totally disintegrated brittle rocks is similarly narrow for most common rock types. Therefore, a possible explanation for the statistical uniformity of sonic-log fluctuations could lie in a similarly uniform distribution of micro- and macrofractures and related porosities within the upper crystalline crust (Scholz *et al.* 1993; Crampin 1994).

The effects of fractures on seismic velocity are governed by crack-induced porosity and the degree of saturation of these pores. The respective elastic moduli for dry and saturated cracked media can be approximated as (Bourbié, Coussy &

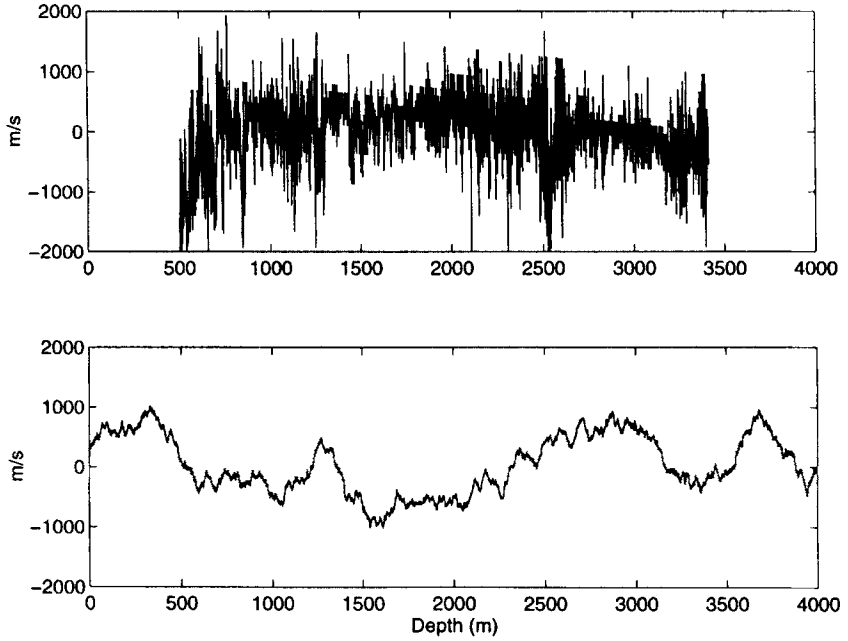

Figure 11. (a) Sonic-log data from Cajon Pass after removing a linear trend defined by a least-squares best fit through the original data, and (b) synthetic data assuming a Hurst number of 0.7 and a correlation scale of 1500 m.

Zinszner 1987)

$$K(\phi) \approx \frac{K_0}{1 + A_1\phi/e}, \qquad \mu(\phi) \approx \frac{\mu_0}{1 + B_1\phi/e} \tag{1a}$$

and

$$K(\phi) \approx \frac{K_0}{1 + A_2\phi}, \qquad \mu(\phi) \approx \frac{\mu_0}{1 + B_2\phi/e}, \tag{1b}$$

where A_1, A_2, B_1 and B_2 are empirical constants with values typically close to unity; K and μ are the bulk and shear moduli as functions of porosity ϕ; K_0 and μ_0 are the shear and bulk moduli when all pore spaces are closed; and e is the aspect ratio of the pore spaces ($\ll 1.0$ for cracks). In the above equations, the porosity is expressed as the fraction of the total considered volume that is occupied by pore spaces. For example, $\phi = 0.1$ implies that pore spaces make up 10 per cent of the total volume. For $A_1 = A_2 = B_1 = B_2 = 1.0$ the respective P-wave velocities for dry and saturated cracked media are thus given by

$$v_p(\phi) \approx \sqrt{\frac{K_0 + 4\mu_0/3}{\rho(1+\phi/e)}} = v_p(\phi = 0)\sqrt{\frac{1}{1+\phi/e}}, \tag{2a}$$

and

$$v_p(\phi) \approx \sqrt{\frac{K_0}{\rho(1+\phi)} + \frac{4\mu_0}{3\rho(1+\phi/e)}}. \tag{2b}$$

Laboratory studies on samples from the KTB boreholes suggest that the theory upon which eqs (1) and (2) are based is adequate to relate crack densities to seismic velocities (Zinke, Gehlen & Berckhemer 1993; J. Zinke, personal communication 1995). Crack-related pores are characterized by small aspect ratios ($e \leq 0.01$; Bourbié *et al.* 1987; Wong, Fredrich & Gwanmesia 1989) and therefore may contribute significantly to the velocity variability observed in sonic logs. Fig. 12(a) shows a hypothetical, synthetic porosity–depth profile with a Hurst number of 0.15, a correlation length of 100 m, an average crack porosity of 0.20 per cent, a standard deviation of the porosity of 0.30 per cent, and a Rayleigh-type probability density function. The cracks are assumed to have a constant aspect ratio e of 0.01. Both the magnitude of the porosities and the average aspect ratio of the cracks represent rather conservative estimates (Bourbié *et al.* 1987; Wong *et al.* 1989). The physical basis of this hypothetical porosity distribution is the empirically observed fractal nature and Rayleigh- or lognormal-type distributions of crack apertures (Wong *et al.* 1989).

Using eqs (1) and (2) and assuming that crack porosity is the only cause of small-scale velocity variations, the random porosity distribution of Fig. 12(a) has been transformed into the velocity distributions corresponding to dry (Fig. 12b) and saturated (Fig. 12c) cracked media. These velocity fluctuations can again be modelled by a von Kármán autocovariance function with a Hurst number of 0.15 to 0.17 and a correlation length of 90 to 110 m. Similar to the observed sonic-log velocity fluctuations (Figs 1, 8a, 8c), these synthetic velocity fluctuations (Figs 12b and 12c) contain abundant negative outliers, which is the direct, and expected, consequence of the $1/\sqrt{x}$-type transformation of the Rayleigh-distributed porosity profile (see eq. 2). The resulting velocity fluctuations are similar in character but have significantly differing standard deviations (approximately 280 m s^{-1} for dry cracks and 120 m s^{-1} for saturated cracks). In reality, one would expect cracks to be neither completely dry nor completely saturated.

DISCUSSION

This study suggests that small-scale cracks may contribute significantly to the stochastic nature of upper-crustal sonic logs. Therefore, an important question to be addressed is whether

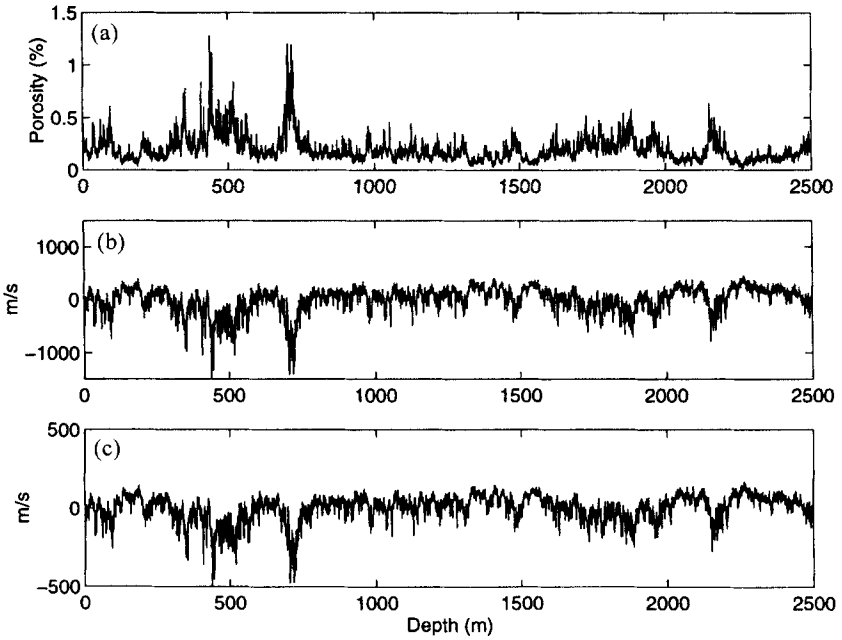

Figure 12. (a) Synthetic crack-porosity profile versus depth with a mean porosity of 0.20 per cent and a standard deviation of 0.30 per cent. The profile has a Hurst number of 0.15 and a correlation length of 100 m. Also shown are the corresponding velocity fluctuations for (b) dry (eq. 2a) and (c) saturated cracks (eq. 2b) assuming constant elastic parameters for the uncracked medium ($K_0 = 59.8$ GPa, $\mu_0 = 35.9$ GPa, $\rho = 2800$ kg m^{-3}).

the crack porosity interpreted from sonic-log variations is representative of larger volumes of rocks or only of the excavation damage zone in the close vicinity of the borehole wall. Hornby (1993) used sonic-log traveltimes recorded over various distance ranges to perform a tomographic reconstruction of the velocity distribution near the borehole wall. He found that in soft sediments, such as clays, there may be low-velocity regions several tens of centimetres thick due to mechanical damage introduced during drilling. Although this excavation damage zone has proved to be much less significant in consolidated sandstones, its potential effects cannot be ignored. One way to assess the importance of the excavation damage zone on the results of this study is to compare sonic-log data recorded with significantly different source–receiver spacings, i.e. penetrations. The only boreholes for which both short ($\sim$1.0 m) and relatively long ($\sim$3.0 m) source–receiver offsets are available are Leuggern and Böttstein. Table 4 compares the second-order statistics of both the short- and the long-offset measurements. In general, the noise level of the long-offset measurements is lower than for the short-offset ones. Otherwise, the measurements are statistically quite similar. This result may indicate that either the excavation damage zone is very thin and thus not important for sonic logs in crystalline rocks, or that it is so thick that it affects short- and long-offset measurements equally.

The separation of deterministic and stochastic components is one of the most controversial and most subjective aspects of stochastic data analysis. In practice, the determination and removal of the deterministic trend is therefore typically guided by the objectives of the subsequent stochastic analysis. An interesting outcome of this study is that the choice of deterministic trend, or rather its maximum frequency content, critically affects the estimates of the correlation length and the standard deviation of the velocity fabric, but not the Hurst number (Table 2). Therefore, the Hurst number, or equivalently the slope of the power spectrum, seems to be a robust parameter, which can be directly compared to the results of other studies regardless of filtering or conditioning of the original sonic-log data. As outlined above, the analyses of the KTB data by Wu *et al.* (1994) and Kneib (1995) are consistent with the low Hurst numbers found in this study. Recently, power spectral slopes corresponding to uniformly low Hurst numbers ($\sim$0.1–0.2) were reported for sonic logs from numerous upper-crustal drill sites in Japan (Sato & Shiomi 1995; H. Sato, personal communication 1995). Finally, and possibly most remarkably, Walden & Hosken's (1985) analyses of sonic logs from a wide variety of sedimentary basins also provided Hurst numbers of similar magnitude and uniformity to those in this study. Stochastic signals with such low Hurst numbers ($\sim$0.0–0.2) are commonly referred to as '$1/k$-' or 'flicker noise', which is a ubiquitous but poorly understood characteristic of a wide variety of dynamic phenomena (e.g. electric noise, stock market fluctuations, traffic jams). Exploring the origin of this flicker-noise nature of sonic-log data should therefore be a major objective of future research.

CONCLUSIONS

Small-scale *P*-wave velocity fluctuations recorded on sonic logs from 10 boreholes drilled in six tectonic environments in Europe and North America have been analysed. These boreholes penetrate the first few kilometres of upper crystalline crust in which the geological age, tectonic evolution, and lithological composition vary significantly. Surprisingly, this geological variability is not reflected in the statistics of the velocity variations measured by the sonic logs. After removing deterministic large-scale trends, the residual small-scale velocity variations of all sonic logs have quasi-Gaussian probability density functions and closely resemble each other in terms of their second statistical moments, i.e. their autocovariance functions. These autocovariance functions can be modelled by so-called von Kármán functions, which characterize band-limited self-affine media. The removal of higher-frequency trends results in systematic reductions of the correlation lengths and standard deviations of the stochastic velocity variations, but leaves the Hurst numbers and the standard deviations of the white noise essentially unaffected.

The similarity of sonic-log velocity variations in widely differing types of upper crystalline crust may be attributed to the intrinsic variability of seismic velocities documented by petrophysical studies, and/or to crack-related porosity. Although it is not possible to establish the importance of the respective contributions on the basis of the available data, the statistical uniformity of the sonic-log variations regardless of the probed lithologies, as well as the fact that the velocity distributions are systematically skewed toward small values, may argue in favour of the dominance of fracturing effects. Fracturing is a common phenomenon throughout the upper crystalline crust, and there is evidence that fractures obey similar geometric and statistical laws regardless of lithological composition and tectonic history. Although total pore space related to cracks is typically volumetrically small, cracks have potentially large effects on the elastic parameters due to their planar geometry. Therefore, it is tentatively suggested that crack-related porosities may at least partially explain the statistical nature and uniformity of sonic-log velocity fluctuations in crystalline rocks.

Table 4.

Borehole	ν	a (m)	σ_h (m/s)	σ_n (m/s)
Leuggern				
Short tool	0.14	60	317	66
Long tool	0.15	68	302	49
Böttstein				
Short tool	0.12	80	370	71
Long tool	0.14	93	364	52

ACKNOWLEDGMENTS

I wish to thank Nagra (National Cooperative for the Disposal of Radioactive Waste), KTB (German Continental Deep Drilling Program), Christopher Juhlin, Bernd Milkereit, and Peter Leary for providing the sonic-log data upon which this paper is based. Peter Leary also provided me with some useful references. Once again, I am grateful to John Goff for enlightening suggestions concerning stochastic signal analysis. I profited from discussions with Wilfried Albert, Philip Birkhäuser, and Peter Blümling, all of Nagra. In-house reviews by Keith Evans, Alan Green, and Johan Robertsson and proof-reading by Carey Sargent improved the earlier versions of this manuscript. I am indebted to Guido Kneib for an exceptionally thorough and constructive review of this paper. ETH-Geophysics Contr. No. 866.

REFERENCES

Bendat, J.S. & Piersol, A.G., 1986. *Random Data,* John Wiley & Sons, New York, N.Y.

Bourbié, T., Coussy, O. & Zinszner, B., 1987. *Acoustics of Porous Media,* Editions Technip, Paris.

Burlini, L. & Fountain, D.M., 1993. Seismic anisotropy of metapelites from the Ivrea–Verbano zone and Serie dei Laghi (northern Italy), *Phys. Earth Planet. Inter.,* **78,** 301–317.

Chatfield, C., 1980. *The Analysis of Time Series: An Introduction,* Chapman & Hall, London.

Christensen, N.I., 1979. Compressional wave velocities in rocks at high temperatures and pressures, critical thermal gradients and crustal low-velocity zones, *J. geophys. Res.,* **84,** 6849–6857.

Crampin, S., 1994. The fracture criticality of crustal rocks, *Geophys. J. Int.,* **118,** 428–438.

Franke, W., 1989. The geological framework of the KTB drill site, Oberpfalz, in *The German Continental Deep Drilling Program (KTB),* pp. 37–54, eds Emmermann, R. & Wohlenberg, J., Springer, Berlin.

Frankel, A. & Clayton, R.W., 1986. Finite difference simulations of seismic wave scattering: implications for the propagation of short-period seismic waves in the crust and models of crustal heterogeneity, *J. geophys. Res.,* **91,** 6465–6489.

Goff, J.A. & Jordan, T.H., 1988. Stochastic modeling of seafloor morphology: Inversion of sea beam data for second order statistics, *J. geophys. Res.,* **93,** 13 589–13 608.

Hansen, B.T., Teufel, S. & Ahrendt, H., 1989. Geochronology of the Moldanubian-Saxothuringian transition zone, northeast Bavaria, in *The German Continental Deep Drilling Program (KTB),* pp. 55–65, eds Emmermann, R. & Wohlenberg, J., Springer, Berlin.

Holliger, K. & Levander, A., 1994a. Structure and seismic response of extended continental crust: Stochastic analysis of the Strona-Ceneri and Ivrea Zones, Italy, *Geology,* **22,** 79–82.

Holliger, K. & Levander, A., 1994b. Seismic structure of gneissic/granitic upper crust: geological and petrophysical evidence from the Strona–Ceneri Zone (northern Italy) and implications for crustal seismic exploration, *Geophys. J. Int.,* **119,** 497–510.

Holliger, K., Green, A.G. & Juhlin, C., 1996. Stochastic analysis of sonic logs from the upper crystalline crust: Methodology, *Tectonophysics,* in press.

Hornby, B.E., 1993. Tomographic reconstruction of near-borehole slowness using refracted borehole sonic arrivals, *Geophysics,* **58,** 1726–1738.

Hurich, C.A. & Smithson, S.B., 1987. Compositional variation and the origin of deep crustal reflections, *Earth Planet. Sci. Lett.,* **85,** 416–426.

Juhlin, C., 1990. Interpretation of reflections in the Siljan Ring area based on results from the Gravberg-1 borehole, *Tectonophysics,* **173,** 345–360.

Kneib, G., 1995. The statistical nature of the upper continental crystalline crust derived from *in situ* seismic measurements, *Geophys. J. Int.,* **122,** 594–616.

Leary, P.C., 1991. Deep borehole evidence for fractal distribution of fractures in crystalline rock, *Geophys. J. Int.,* **107,** 615–627.

Levander, A., Hobbs, R.W., Smith, S.K., England, R.W., Snyder, D.B. & Holliger, K., 1994. The crust as a heterogeneous 'optical' medium, or 'crocodiles in the mist', *Tectonophysics,* **232,** 281–297.

Li, X.-P. & Haury, J.C., 1995. Characterization of heterogeneities from sonic velocity measurements using the wavelet transform, *Exp. Abst. 65th Ann. Meet. Soc. Expl. Geophys., Houston, Texas,* pp. 488–491.

Mandelbrot, B.B., 1983. *The Fractal Geometry of Nature,* Freeman, New York, NY.

Milkereit, B., Green, A., Wu, J. & Adam, E., 1994. Integrated seismic and borehole study of the Sudbury igneous complex, *Geophys. Res. Lett.,* **21,** 931–934.

Moos, D. & Zoback, M.D., 1983. In situ studies of velocity in fractured crystalline rocks, *J. geophys. Res.,* **88,** 2345–2358.

Mueller, St., 1977. A new model of the continental crust, in *The Earth's Crust: Its Nature and Physical Properties,* ed. Heacock, J.G., Am. Geophys. Un. Geophys. Monogr. Ser., **20,** 289–317.

North, C.P. & Halliwell, D.I., 1994. Bias in estimating fractal dimension with the rescaled-range (R/S) technique, *Mathematical Geology,* **26,** 531–555.

Paillet, F.L. & White, E.J., 1982. Acoustic modes of propagation in the borehole and their relationship to rock properties, *Geophysics,* **47,** 1215–1228.

Pilkington, M. & Todoeschuck, J.P., 1991. Naturally smooth inversions with a priori information from well logs, *Geophysics,* **56,** 1811–1818.

Salisbury, M.H., Iuliucci, R. & Long, C., 1994. Velocity and reflection structure of the Sudbury Structure from laboratory measurements, *Geophys. Res. Lett.,* **21,** 923–926.

Sato, H. & Shiomi, K., 1995. Power law spectra of well-log data in Japan, *IUGG Abstracts,* **B,** 408.

Scholz, C.H., Dawers, N.H., Yu, J.Z., Anders, M.H. & Cowie, P.A., 1993. Fault growth and fault scaling laws: Preliminary results, *J. geophys. Res.,* **98,** 21 951–21 961.

Serra, O., 1984. *Fundamentals of Well-Log Interpretation – 1. Acquisition of Logging Data,* Elsevier, Amsterdam.

Silver, L.T. & James, E.W., 1988. Geologic setting and lithologic column of the Cajon Pass deep drillhole, *Geophys. Res. Lett.,* **15,** 941–944.

Telford, W.M., Geldart, L.P. & Sheriff, R.E., 1990. *Applied Geophysics,* 2nd edn, Cambridge University Press, Cambridge.

Thury, M., Gautschi, A., Mazurek, M., Müller, W.H., Naef, H., Pearson, F.J., Vomvoris, S. & Wilson, W., 1994. *Geology and Hydrology of the Crystalline Basement of Northern Switzerland,* Nagra Technical Report 93-01, Nagra, Wettingen.

Todoeschuck, J.P. & Jensen, O.G., 1988. Joseph geology and seismic deconvolution, *Geophysics,* **53,** 1410–1414.

Turcotte, D.L., 1992. *Fractals and Chaos in Geology and Geophysics,* Cambridge University Press, Cambridge.

von Kármán, T., 1948. Progress in the statistical theory of turbulence, *J. Mar. Res.,* **7,** 252–264.

Walden, A.T. & Hosken, J.W.J., 1985. An investigation of the spectral properties of primary reflection coefficients, *Geophys. Prospect.,* **33,** 400–435.

White, D.J., Milkereit, B., Wu, J.J., Salisbury, M.H., Mwenifumbo, J., Berrer, E.K., Moon, W. & Lodha, G., 1994. Seismic reflectivity of the Sudbury structure north range from borehole logs, *Geophys. Res. Lett.,* **21,** 935–938.

Wong, T.-F., Fredrich, J.T. & Gwanmesia, G.D., 1989. Crack aperture statistics and pore space fractal geometry of Westerly Granite and Rutland Quartzite: implications for elastic contact model of rock compressibility, *J. geophys. Res.,* **94,** 10 267–10 278.

Wu, R.-S. & Aki, K., 1985. The fractal nature of inhomogeneities in the lithosphere evidenced from seismic wave scattering, *Pure appl. Geophys.,* **123,** 805–818.

Wu, R.-S. & Aki, K., 1988. Introduction: seismic wave scattering in a three-dimensionally heterogeneous earth, *Pure appl. Geophys.*, **128**, 1–6.

Wu, R.-S., Xu, Z. & Li, X.-P., 1994. Heterogeneity spectrum and scale-anisotropy in the upper crust revealed by the German continental deep-drilling (KTB) holes, *Geophys. Res. Lett.*, **21**, 911–914.

Wyllie, M.R.J., Gregory, A.R. & Gardener, L.W., 1956. Elastic wave velocities in heterogeneous and porous media, *Geophysics*, **21**, 41–70.

Zinke, J., Gehlen, K. & Berckhemer, H., 1993. Imagery of open microcracks for the statistical analysis. Comparison with elastic anisotropy, *KTB-Report*, **93-2**, 235–237.

APPENDIX A: STOCHASTIC ANALYSIS OF SONIC-LOG DATA

Data model

The basis for this analysis is a separation of the velocity–depth function $V(z)$ observed in the sonic logs into a deterministic part $V_0(z)$ and a stochastic part $s(z)$:

$$V(z) = V_0(z) + s(z). \tag{A1}$$

The deterministic part of the velocity–depth function is generally considered to be known, for example from wide-angle seismic measurements. Analysis of the small-scale stochastic fluctuations of the sonic log is based on the approach described by Goff & Jordan (1988). Methodological and algorithmic details of the corresponding adaptation to sonic-log data are given by Holliger *et al.* (1996), and therefore only a summary of the most relevant aspects is given here.

A key assumption of this technique is that a sonic log is a linear system. Small-scale fluctuations may then be represented as a statistical data sequence consisting of noise $n(z)$ plus the actual *in situ* velocity fluctuations along the borehole filtered by the system response of the logging tool:

$$s(z) = f(z) * h(z) + n(z). \tag{A2}$$

Under this assumption, the dominant effect of the logging response $f(z)$ is the averaging of the *in situ* velocity fabric $h(z)$ over the minimum source–receiver spacing of the tool (Serra 1984). The logging system filter $f(z)$ thus represents some form of a low-pass filter with a spatial cut-off frequency close to 1/(averaging interval of the sonic tool). Here, $f(z)$ is approximated by a running-mean filter with a window length corresponding to the minimum source–receiver spacing of the sonic tool. This corresponds to the expected system response of an uncompensated sonic tool. How well this basic low-pass filter approximates the filtering effects of compensated tools or modern sonic array tools is, however, difficult to assess, since the geometry of the active sources and receivers and the averaging procedure used to calculate the velocity at each observation point are often only known to the contractor.

Second-order statistics

Analogous to variations in sea-floor topography (Goff & Jordan 1988), velocity fluctuations in sonic logs would probably fail formal tests of normality. In practice, however, their probability distribution can be approximated as Gaussian. Thus, sonic-log fluctuations are characterized well by their second statistical moments, i.e. their autocovariance functions or, equivalently, their power spectra. In this study a 'biased' estimator was used to calculate the autocovariance function and therefore the value at zero lag corresponds to the variance of the process (Bendat & Piersol 1986). For white system noise $n(z)$, the autocovariance function of $s(z)$ is given by

$$C_{ss}(\zeta) = C_{ff}(\zeta) * C_{hh}(\zeta) + \sigma_n^2 \delta(\zeta), \tag{A3}$$

where ζ is the lag, σ_n^2 is the variance of the white system noise, $\delta(\zeta)$ is the delta function, and $C_{ss}(\zeta)$, $C_{hh}(\zeta)$, and $C_{ff}(\zeta)$ are the respective autocovariance functions of the observed sonic-log velocity variations, the actual *in situ* velocity variations along the borehole wall, and the system filter (Goff & Jordan 1988; Holliger *et al.* 1996). Note that $f(z)$ and thus $C_{ff}(\zeta)$ are assumed to be known. The total variance σ_s^2 of $s(z)$, and thus the trade-off between σ_h^2 and σ_n^2, is given by

$$\sigma_s^2 = C_{ss}(0) = \sigma_h^2 + \sigma_n^2, \tag{A4}$$

where σ_h^2 and σ_n^2 are the respective variances of the *in situ* velocity fluctuations along the borehole wall and the noise present in the sonic-log data. In reality, noise is unlikely to be completely white and the decision to model this end-member-type noise is essentially an expression of the lack of knowledge of the detailed character of noise in sonic logs. However, since the noise correlation length is expected to be much shorter (say a few measurement intervals or 0.5 to 1.0 m) than that of the velocity fluctuations (at least a few tens of metres) eqs (A3) and (A4) may provide a reasonable minimum estimate of the total amount of noise present in the data. Following Goff & Jordan (1988) the variance of the white noise σ_n^2 is thus estimated by taking the difference between the first two samples of C_{ss}.

Parametric model of the autocovariance function of crustal seismic heterogeneity

In order to quantify the small-scale velocity fluctuations $h(z)$, a parametrized model of the corresponding autocovariance function $C_{hh}(\zeta)$ is required. During the past decade, the scale independence and associated self-affine or fractal geometry of many natural phenomena have received significant attention (Mandelbrot 1983; Turcotte 1992). The von Kármán autocovariance function characterizes a family of stochastic processes that are self-affine at scales smaller than the correlation length a:

$$C_{hh}(\zeta) = \frac{\sigma_h^2}{2^{\nu-1}\Gamma(\nu)} (\zeta/a)^{\nu} K_{\nu}(\zeta/a), \tag{A5}$$

where ν is the Hurst number, Γ is the gamma function, and K_{ν} is the modified Bessel function of the second kind of order $0 < \nu \leq 1$. The fractal dimension D is related to the Hurst number ν by $D = E + 1 - \nu$ (Goff & Jordan 1988). In the case of a stochastic data sequence, the Euclidean dimension E is one, so D lies between 1.0, a very smooth sequence, and 2.0, a very rough sequence.

The Fourier transform of eq. (A5) corresponds to the power spectrum of the stochastic process $h(z)$. In E dimensions it is given by (Goff & Jordan 1988)

$$P_{hh}(k) = \frac{\sigma_h^2 (2\sqrt{\pi}a)^E \Gamma(\nu + E/2)}{\Gamma(\nu)(1 + k^2 a^2)^{\nu + E/2}}, \tag{A6}$$

where k is the wavenumber. For $ka \ll 1$ $P_{hh}(k)$ thus corresponds to a white spectrum, whereas for $ka \gg 1$ it decays in proportion to $k^{-(2\nu+E)}$. The latter is referred to as power-law behaviour (Turcotte 1992), which is typical of random fractal phenomena.

The transition from a white to a power-law spectrum occurs around $ka \approx 1$. Many scientists work with pure power-law processes ($k^{-\beta}$ fall-off of the power spectrum over the entire wavenumber range), which are mathematically quite awkward (Pilkington & Todoeschuck 1991). Moreover, the power-law behaviour of natural phenomena normally does not extend beyond a certain lower wavenumber limit. Partially because of its band-limiting property, the von Kármán family of autocovariance functions has proved to be a useful and versatile tool for describing a wide variety of fractal phenomena, such as turbulence (von Kármán 1948), sea-floor morphology (Goff & Jordan 1988), and crustal seismic heterogeneity (Wu & Aki 1985; Frankel & Clayton 1986; Holliger & Levander 1994a,b; Levander *et al.* 1994).

Inversion of sonic-log velocities for small-scale seismic structure

Eqs (A1) to (A5) provide the information required to invert $s(z)$ for the second-order statistics of the actual *in situ* velocity fluctuations, that is $C_{hh}(\zeta)$:

(1) after removing the deterministic trend, evaluate the autocovariance function $C_{ss}(\zeta)$ of the stochastic part of the sonic-log variations $s(z)$ and take the second sample as the variance of the process $C_{ss}(i=2) \approx \sigma_h^2$;

(2) make educated guesses for ν based on the slope of the power spectrum, and for a from the distance to the first zero-crossing of the autocovariance function (Goff & Jordan 1988; Wu *et al.* 1994);

(3) limit the maximum considered lag of the observed autocovariance function $C_{ss}^{\text{obs}}(\zeta)$ to three times the initial guess of the correlation length a;

(4) calculate the corresponding von Kármán function $C_{hh}(\zeta)$ and filter it with the autocovariance function $C_{ff}(\zeta)$ of the system filter $f(z)$—this yields the calculated value of $C_{ss}(\zeta) \equiv C_{ss}^{\text{calc}}(\zeta)$;

(5) adjust a and ν to minimize the misfit between the observed and calculated autocovariance functions $|C_{ss}^{\text{obs}}(\zeta) - C_{ss}^{\text{calc}}(\zeta)|$ using a standard least-squares method.

The choice of the system filter $f(z)$ influences the decay rate of $C_{ss}^{\text{calc}}(\zeta)$ near zero lag and thus may affect the estimated value of the Hurst number ν. Since the nature of the system filter is not yet fully understood for sonic-log data, all Hurst number estimates were verified by independent analysis of the slopes of the corresponding power spectra. In the spectral domain, low-pass filtering effects of the system response are only present at very high wavenumbers (Fig. 9) and thus can be easily isolated and excluded from the analysis (Goff & Jordan 1988).